Available online at www.sciencedirect.com
ScienceDirect
Tetrahedron
Tetrahedron 63 (2007) 3457–3464

A perylenedicarboxamide linker for DNA hairpins

Frederick D. Lewis,* Ligang Zhang,† Richard F. Kelley, David McCamant‡ and Michael R. Wasielewski*

Department of Chemistry, Northwestern University, Evanston, IL 60208-3113, United States

Received 24 July 2006; revised 22 October 2006; accepted 23 October 2006
Available online 2 February 2007

Abstract—The synthesis and properties of a perylenediamide diol linker and several DNA hairpins possessing this linker are described. The diol linker absorbs and fluoresces strongly in the visible. Hairpins having poly(dA)–poly(dT) stems have fluorescence quantum yields and decay times similar to those of the linker, indicating that hole injection does not occur from the singlet excited linker into the base pair domain. Fluorescence quenching by dG or dZ bases is observed when these bases are located near the linker. The strong distance dependence of fluorescence quenching is consistent with a superexchange mechanism for electron transfer. Failure to observe formation of the linker anion radical by means of femtosecond time resolved absorption spectroscopy is attributed to fast charge recombination. The properties and behavior of the perylene linker and its hairpins are compared to those of other arenedicarboxamide linkers.

1. Introduction

Fluorescent nucleoside analogs have been widely used as probes of nucleic acid structure and properties. Several approaches to the introduction of a fluorescent chromophore into duplex DNA have been developed. These include the use of fluorescent nucleobase analogs such as aminopurine[1,2] or aromatic nucleosides,[3,4] which replace one or both members of base pair, covalent modification of a nucleobase with an appended chromophore, which protrudes into the major or minor groove,[5–9] and 5′- or 3′-terminal appendage of a fluorophore, which serves as a hydrophobic capping group.[10,11]

The use of arenedicarboxamide linkers for the preparation of bis(oligonucleotide) conjugates was introduced by Letsinger and co-workers.[12,13] They found that conjugates having terephthalamide or 4,4′-stilbenedicarboxamide (TPA and SA, Chart 1) linkers with short poly(dA)–poly(dT) 'arms' form folded hairpin structures, rather than extended duplex structures. We and others have reported the synthesis and properties of numerous hairpin structures having a variety of arenedicarboxamide[14–16] and the naphthalene and perylene bis(arenedicarboximide) linkers NDI and PDI (Chart 1).[17] The remarkable stability of synthetic hairpins possessing short base pair stems is a consequence of hydrophobic π-stacking interactions with the adjacent base pair and the entropic advantage provided by a linker of appropriate dimensions.[18] Molecular modeling of hairpins having SA linkers indicates that the propyl side chains are sufficiently long to permit π-stacking while providing conformational flexibility in the hairpin loop region.[19] While other linkers including oligo(ethylene glycols) and disulfides have been employed in the preparation of hairpin-forming conjugates,[20,21] these hairpins do not display significant thermodynamic stabilization when compared to natural hairpin loops composed of several nucleotides.[22]

Synthetic hairpins having arenedicarboxamide and diimide linkers (Chart 1) have been employed in studies of DNA photoinduced electron transfer.[14,23–26] The singlet excited state of the linker serves as an electron acceptor in these reactions and the base pair domain as the electron donor (hole acceptor). The fluorescence of the DPA, NI, and PDI-linkers in hairpins with poly(dA)–poly(dT) base pair domains is completely quenched, indicative of highly efficient hole injection into the poly(dA) domain.[17,27–31]

All of the arenedicarboxamide linkers reported to date have absorption bands in the UV spectral region. A number of applications, including single molecule spectroscopic studies and fluorescent labeling of cellular DNA would benefit from the availability of a linker, which absorbs strongly in the visible and has a high fluorescence quantum yield. We have recently reported the use of a new perylenedicarboxamide

Keywords: Fluorescence quenching; Electron transfer; Hole injection; Arenedicarboxamide; Circular dichroism.
* Corresponding authors. Tel.: +1 847 491 3441; fax: +1 847 467 2184; e-mail addresses: fdl@northwestern.edu; wasielew@chem.northwestern.edu
† Present address: Chemistry Division, Argonne National Laboratory, Argonne, IL 60439, United States.
‡ Present address: Department of Chemistry, University of Rochester, Rochester, NY 14627, United States.

0040–4020/$ - see front matter © 2007 Elsevier Ltd. All rights reserved.
doi:10.1016/j.tet.2006.10.089

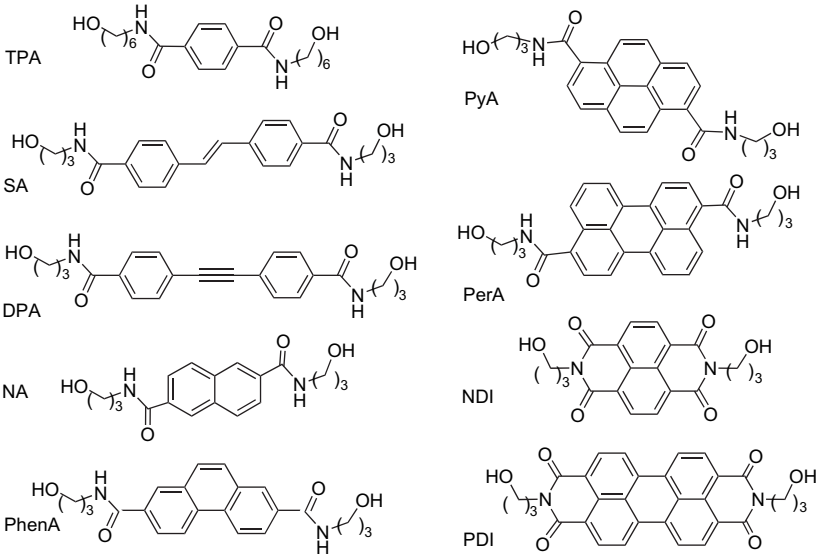

Chart 1. Structures of the arenedicarboxamide and bis(dicarboximide) diol linkers.

linker (PerA, Chart 1) as an acceptor in our studies of the orientation dependence of fluorescence resonance energy transfer (FRET).[32] Unlike the more widely used PDI linker, which is a powerful electron acceptor and thus not suited for use as a fluorescent probe in DNA conjugates,[17,31] PerA is strongly fluorescent except when π-stacked with guanine. We report here the synthesis and properties of the PerA linker and several of its hairpin conjugates. These properties are compared to those of the SA,[33] DPA,[27] NA,[34] PhenA,[35] and PyA[36] linkers that we have studied previously (Chart 1).

2. Results and discussion

2.1. Synthesis and properties of the perylenediamide linker

The diamide diol linkers SA, DPA, NA, PhenA, and PyA have all been prepared via the two step procedure of Letsinger for conversion of the corresponding diacid to the diacid chloride followed by reaction of the diacid chloride with 3-hydroxypropylamine.[37,13] The starting material for the preparation of PerA was the perylenedicarboxylic acid diisobutyl ester, which was purchased as the 3,9-isomer. It was converted directly to the PerA linker via the cyanide-catalyzed reaction with 3-hydroxypropylamine following the procedure of Högberg (see Section 4).[38] Whereas both the diester and the diamide have spectral properties consistent with the presence of a single isomer, the DNA conjugates prepared from the diamide (vide infra) were obtained as ca. 1:1 mixtures of isomers attributed to the presence of both 3,9- and 3,10-isomers in the commercial material, a conclusion later confirmed by the supplier. Thus the properties of the PerA linker are those of the isomer mixture.

The absorption and fluorescence spectra of PerA in methanol are shown in Figure 1. Spectral data are reported in Table 1 along with data for other dicarboxamide linkers. Both the absorption and fluorescence spectra of PerA are broadened and red-shifted compared to those of unsubstituted perylene.[39] The long wavelength absorption band of perylene is attributed to an essentially pure, allowed HOMO–LUMO transition, which is long-axis polarized.[40,41] The fluorescence quantum yield and decay time of PerA are similar to those for perylene (Φ_{fl}=0.94 and τ_S=6.4 ns in cyclohexane).[39] The fluorescence quantum yield is the largest of any arenedicarboxamide studied to date (Table 1).

The femtosecond transient absorption spectrum of PerA is shown in Figure 2. It consists of a broad band centered at 690 nm and a negative band extending from 550 nm to shorter wavelengths. The former, attributed to $S_1 \rightarrow S_n$ absorption of PerA, is blue-shifted and broader than the corresponding transient absorption band for perylene (λ_{max}=710 nm).[42] The latter is attributed to overlapping stimulated emission (ca. 500 nm) and ground state bleach (ca. 450 nm). Both the positive and negative bands have

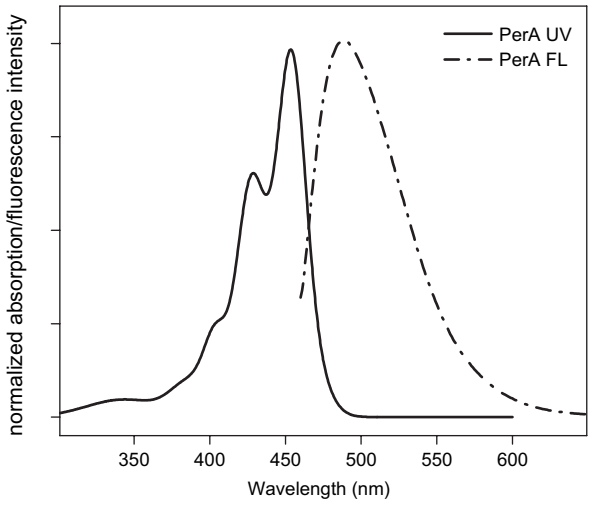

Figure 1. Absorption and fluorescence spectra of PerA in methanol (ca. 20 μM).

Table 1. UV absorption (maxima and absorbance), fluorescence (maxima, quantum yields, and lifetimes), and reduction potentials (ground and excited states) of the arenedicarboxamide linkers (Chart 1)

Linker	λ_{abs}, nm (log A)	λ_{fl}, nm	Φ_{fl}	τ_S, ns	E_S, eV	$-E_{red}$, V[g]	E^*_{red}
SA[a]	328 (4.45)	385	0.17	0.39	3.35	1.91	1.44
DPA[b]	305 (4.81)	351	0.33	0.22	3.76	1.98	1.78
NA[c]	340 (3.41), 296 (4.36)	373	0.56	12.0	3.55	2.05	1.50
PhenA[d]	370 (2.30), 303 (2.40)	374	0.48	18	3.35	2.03	1.32
PyA[e]	380 (3.52), 350 (4.52)	364	0.38	19	3.26	1.75	1.51
PerA[f]	453 (4.18)	489	0.93	5.9	2.70	1.37	1.33

[a] Data from Ref. 33.
[b] Data from Ref. 27.
[c] Data from Ref. 34.
[d] Data from Ref. 35.
[e] Data from Ref. 36.
[f] Current work.
[g] Reduction potentials measured in DMF and reported versus SCE.

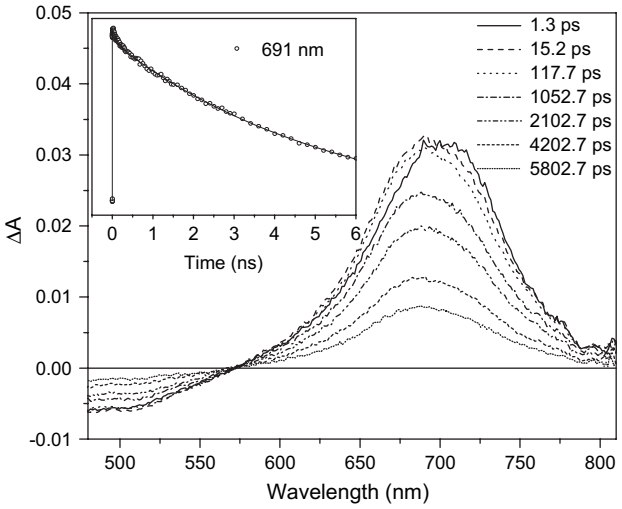

Figure 2. Transient absorption spectra of PerA in methanol (ca. 10 μM) following excitation with 414 nm, 120 fs laser pulses. Inset: transient absorption kinetics at 691 nm of PerA following 414 nm, 120 fs laser pulses. Nonlinear least-squares fit to the 1 ps–5.8 ns data is also shown.

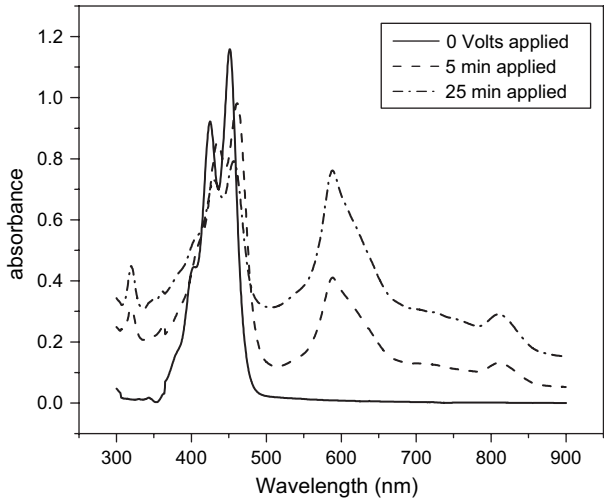

Figure 3. Spectroelectrochemistry of PerA in DMSO (ca. 70 μM). Applied voltage −1.8 V.

decay times similar to the PerA fluorescence decay time (Table 1).

The cyclic voltammogram for PerA in dimethyl formamide (DMF) displayed two reversible reduction waves. The one-electron reduction potentials for PerA and the other diamides reported in Table 1 are referenced to SCE using ferrocene as an internal redox standard. The absorption spectrum of the anion radical $PerA^-$ obtained by means of spectroelectrochemistry in DMSO consists of a strong band at 595 nm (Fig. 3), similar in appearance to that reported for the perylene anion radical by Knibbe et al.[43]

2.2. Synthesis and structure of DNA conjugates

PerA was converted to its mono-protected, monoactivated derivative by sequential reaction with dimethoxytrityl chloride to provide the mono-DMT derivatives followed by reaction with 2-cyanoethyl diisopropylchlorophosphoramidite. The modified linker was incorporated into bis(oligonucleotide) conjugates (Chart 2) by means of conventional phosphoramidite chemistry using an Expedite synthesizer, following the procedure of Letsinger and Wu.[37] Conjugates **1**–**7** containing the PerA linker appeared as two closely-spaced peaks on HPLC, designated as **a** and **b** on the basis of retention time. The two peaks for conjugates **1**–**4** were separated by HPLC and found to have identical mass spectra and similar UV and CD spectra and 260 nm melting temperatures. The long wavelength bands of the UV spectra have the same vibronic structure as PerA (Fig. 1) indicating that the hairpins do not form co-facial dimers, as has been observed for perylene diimide linked hairpins.[31] The melting temperature of conjugates **1a** and **1b** is 62 °C, similar to that for SA and PhenA linked hairpins having the same base pair stem. T_M values for conjugates **2**–**4** (separate peaks) and **5**–**7** (mixture of peaks) are 66±1 °C; their higher values when compared to **1** reflect the greater stability of a dG–dC or dZ–dC base pair versus a dA–dT base pair.[44]

The CD spectra of conjugates **1a** and **1b** are shown in Figure 4. Both display peaks in the 200–300 nm spectral region similar to that of poly(dA)–poly(dT), characteristic of A-tract duplexes.[45] No induced CD band is observed for the PerA linker in the 400–500 nm spectral region, suggesting that its electronic transition dipole is aligned with the long-axis of the adjacent base pair.[46] The fluorescence excitation and emission spectra of **1a** and **1b** are shown in Figure 5. Both excitation spectra are similar to the absorption spectrum of PerA; however, the emission spectrum of **1a** is

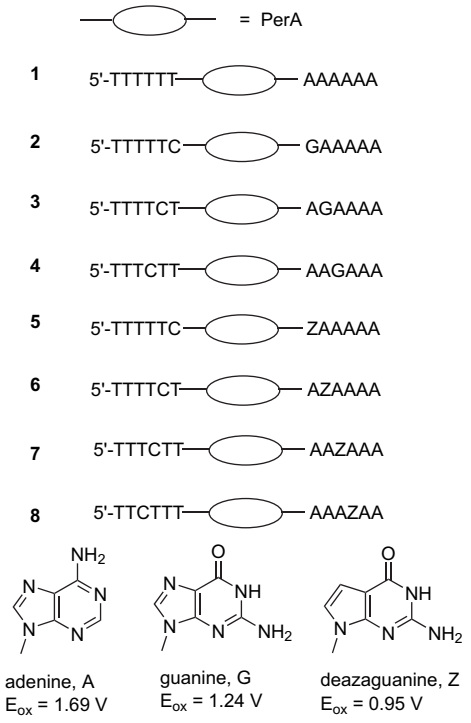

Chart 2. Base sequences for PerA-linked hairpins **1**–**8** and structures for the purine bases.

less structured than that of **1b** and the former has a slightly longer singlet decay time (τ_S=6.8 ns vs 6.1 ns). The fluorescence emission spectrum of a mixture of **1a** and **1b** resembles the sum of the component spectra, having a flattened top rather than the symmetric band shape of PerA (Fig. 1).

The conjugates **1a** and **1b** are assigned to hairpins possessing 3,9- and 3,10-perylenedicarboxamide linkers on the basis of their spectral properties and the propensity of pyrene to form mixtures of isomeric diesters.[47] We have not attempted to assign a specific linker isomer to conjugates **1a** and **1b**. Since the structures and properties of the diamides are similar,

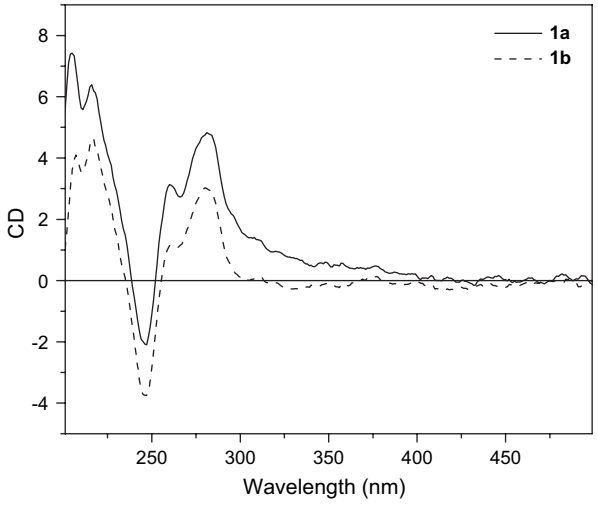

Figure 4. CD spectra of hairpins **1a** and **1b** (ca. 10 μM in 10 mM sodium phosphate, pH 7.2, with 0.1 M NaCl). Spectra are average of 10 scans with base-line correction using the buffer solution.

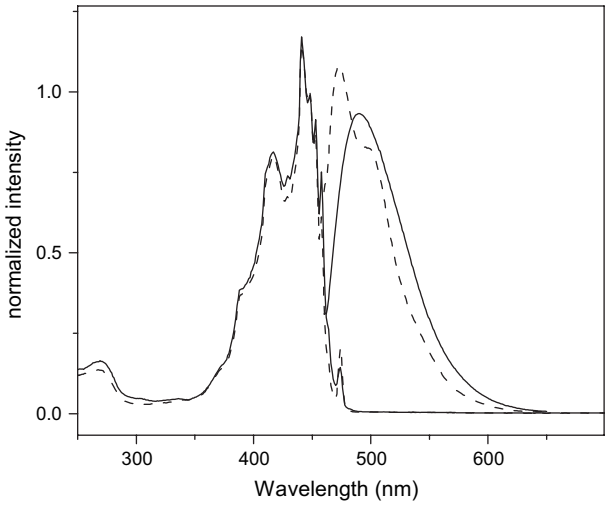

Figure 5. Fluorescence excitation and emission spectra of hairpins **1a** (solid lines) and **1b** (dashed lines) in aqueous solution (ca. 5 μM in 10 mM sodium phosphate, pH 7.2, with 0.1 M NaCl). Sharp features in the excitation spectrum are attributed to noise for the highly dilute samples.

their separation is not considered essential in all applications and was not undertaken for conjugates **5**–**8**.

2.3. Excited state behavior

Fluorescence quantum yield and lifetime data for the PerA-linked hairpins are reported in Table 2. The high value of Φ_{fl} and absence of short lived decay components in either the fluorescence or transient absorption spectra of **1** indicate that ^{1}PerA does not oxidize the adjacent dA–dT base pair.[48] In contrast, extensive quenching is observed for hairpins **2**, **5**, and **6**, which have dG or dZ base located near the linker (Chart 2). The fluorescence decay times of **2** and **6** are similar. The absence of a fast fluorescence decay component for **5** is indicative of quenching that occurs faster than the instrument response ($k_q \geq 10^{11}$ s^{-1}). These results are analogous to those previously observed for the PhenA linker[35] and are consistent with an electron transfer mechanism in which ^{1}PerA is reduced and a neighboring dG or dZ base is oxidized. Relatively weak long-lived fluorescence decay components with decay times similar to that of **1** are observed for **2**, **5**, and **6**. These are attributed to the presence of hairpins lacking dG or dZ bases as trace impurities.

The energetics of photoinduced charge separation and charge recombination processes can be estimated using Weller's equations (Eqs. 1 and 2)

$$\Delta G_{cs} = E_{ox} - E_{red} - E_S + C \quad (1)$$

$$\Delta G_{cr} = E_{red} - E_{ox} \quad (2)$$

where E_S and E_{red} are the PerA singlet energy and reduction potentials (Table 1), E_{ox} is the nucleobase oxidation potential, and C is the solvent-dependent Coulombic attraction energy.[49] Values of E_{ox} for the π-stacked bases in the core of DNA have not been measured but are assumed to be similar to the values for the individual nucleotides in a polar aprotic solvent (Chart 2).[50] The value of C in a moderately polar

Table 2. Fluorescence quantum yields and decay times, transient absorption decay times, and quenching rate constants for PerA-linked hairpins

Hairpin	Φ_{fl}[a]	τ_{fl}, ns[b]			τ_{ta}, ps[c]	10^{-9} k_q, s^{-1}
		a	**b**	**a** and **b**		
1	0.89	6.8	6.1	6.3		
2 (1GC)	0.06	0.30[d]	0.28[d]		270	3.3
3 (2GC)	0.74	5.7	4.5			0.05
4 (3GC)	0.87	6.7	5.7			<0.01
5 (1ZC)	<0.01			6.5[d]	0.8 (87), 21 (13)	1000
6 (2ZC)	0.20			0.20[d]	160	5.4
7 (3ZC)	0.82			5.6		0.02
8 (4ZC)	0.89					

[a] Fluorescence quantum yield for separated isomers or a mixture of **a** and **b**.
[b] Fluorescence decay times (single exponential decay or major components) for separated or combined isomers **a** and **b**.
[c] Decay times obtained from fitting of 700 nm transient absorption decays. A single short lived transient is observed for **2** and **6**. The short lived component of the transient decay of **5** is best fit as a dual exponential (% of decay amplitude). Transient decay components with decay times comparable to or longer than the 3.5 ns time window for these measurements are observed for **1** and **3**–**7**.
[d] Longer lived fluorescence components attributed to small amounts of hairpins lacking G or Z bases are also observed for **2a** and **2b** (5.3 ns, ca. 10%) and for **5** (6.5 ns, 100%) and **6** (6.1 ns, ca. 20%).

environment is sufficiently small that it can be neglected. The calculated values of ΔG_{cs} for oxidation of dA, dG, and dZ for charge recombination, as are shown in Figure 6, are +0.36, −0.09, and −0.38 eV, respectively.

The time resolved transient absorption spectra for **2** are shown in Figure 7. The spectral band shape is similar to that of the PerA linker (Fig. 2), however, the decay times for both the positive and negative bands are much faster for **2**. The agreement of the transient decay times for **2** and **6** with the fluorescence decay times for these hairpins supports the assignment of the transient decay to ^{1}PerA. In the case of **5** two fast decay components are observed, the shorter lived one having the larger amplitude. Its 0.8 ps decay time is consistent with our inability to detect a fast fluorescence decay component. Conspicuous by its absence in the transient spectra is the relatively narrow 595 nm band of $PerA^-$ observed by spectroelectrochemistry (Fig. 3). Evidently, charge recombination of the charge-separated state is sufficiently rapid to prevent detectable accumulation of the transient $PerA^-$ species, as is the case for other dyad systems having relatively low energy singlet charge-separated states.[51,52]

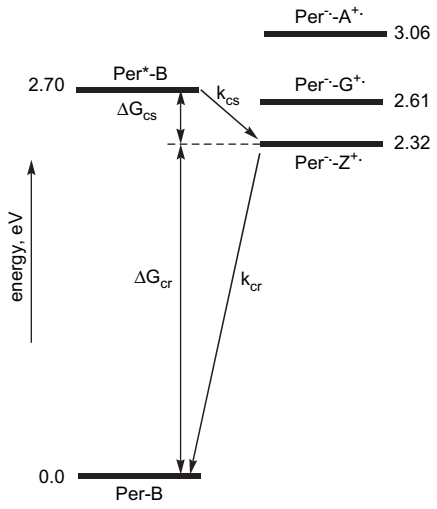

Figure 6. Energy diagram for the PerA singlet state and the $PerA^{-\bullet}/B^{+\bullet}$ ion pair states with the neighboring bases adenine, guanine, and deazaguanine.

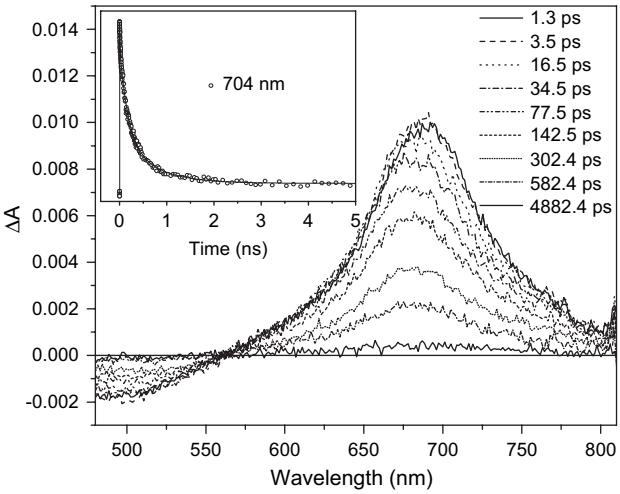

Figure 7. Transient absorption spectra of hairpin **2** in aqueous solution (ca. 10 μM in 10 mM sodium phosphate, pH 7.2, with 0.1 M NaCl) following excitation with 414 nm, 120 fs laser pulses. Inset: transient absorption kinetics at 691 nm of **2** following 414 nm, 120 fs laser pulses. Nonlinear least-squares fit to the data is also shown.

The efficiency of fluorescence quenching and rate constant for charge separation are strongly dependent upon the number of dA–dT base pairs separating PerA and the dG or dZ hole acceptor, little quenching being observed for two or more intervening base pairs. This distance dependence is similar to that observed by Hess et al.[53] for the photoinduced charge transfer using an acridinium hole donor and dG or dZ as hole acceptor. The inability of singlet acridinium or PerA to oxidize dA limits the occurrence of charge separation to a single step superexchange mechanism, which is strongly distance dependent, rather than a hole hopping mechanism, which is weakly distance dependent.[54]

3. Conclusions

The properties of several hairpins having arenedicarboxamide linkers and poly(dA)–poly(dT) stems are summarized in Table 3. For hairpins with the same stem length there is little variation in thermal stability, as indicated by their similar T_M values. Evidently the differences in diamide

Table 3. Melting temperatures, fluorescence quantum yields and decay times, and hole injection mode for poly(dT)–poly(dA) hairpin conjugates

Linker	Stem length	T_M, °C	Φ_{fl}	τ_S, ns[g]	Hole injection[h]
SA[a]	6	59	0.38	0.045 (71), 2.2 (21)	Rev
DPA[b]	5	55	<0.01		Irrev
NA[c]	5	53	0.01	0.31 (90), 3.2 (10)	Rev
PhenA[d]	6	62	0.41	25	None
PyA[e]	6	56	0.37	0.01 (70), 4.5 (16), 8.7 (14)	Rev
PerA[f]	6	62	0.89	6.8	None

[a–f] See Table 1 for literature references.
[g] Values obtained from fluorescence decays. Pre-exponentials in parentheses.
[h] Rev=reversible, irrev=irreversible, none=no hole injection.

dimensions do not have a significant effect on hairpin stability. Hairpins with PerA or PhenA linkers and poly(dA)–poly(dT) stems have fluorescence quantum yields and lifetimes similar to those of the linkers (Table 1), indicative of their inability to inject a hole into the poly(dA) domain. Hairpins having SA, NA, and PyA linkers display multiple exponential fluorescence decay, with short lived components, which are significantly shorter (Table 3) than those for the linkers (Table 1). This behavior has recently been attributed to reversible hole injection into the hairpin base pair domain with charge recombination accounting for the longer lived fluorescence decay components.[48] Hairpins having a DPA dicarboxamide linker or NI or PDI diimide linkers[17] are non-fluorescent as a consequence of rapid, irreversible hole injection into the base pair domain.

Whereas the PerA-oligonucleotide conjugates cannot be used for studies of photochemical hole injection, they are well suited for other applications. Their low UV absorbance in the 300–380 nm spectral region was exploited in our studies of FRET in doubly-labeled capped hairpins having an SA fluorescence donor and PerA fluorescence acceptor.[32] We also envision their use as electron acceptors in doubly-labeled capped hairpins having singlet state electron donors at the opposite end of the base pair domain. The high fluorescence yield, long wavelength absorption, and resistance to quenching by nucleobases (other than a nearest neighbor dG (93% quenching) or second nearest neighbor dG (17% quenching)) make the PerA chromophore potentially useful in studies of cellular DNA.

4. Experimental section

4.1. General methods

UV absorption, fluorescence, and circular dichroism spectra were obtained as previously described on samples contained in 1 cm path length cells.[33] Quantum yields for fluorescence were determined using fluorescein in ethanol as a reference standard (Φ_{fl}=0.79).[55] CD spectra are the average of 10 scans with a data interval of 0.5 nm and a time interval of 2 s per point. The base lines are corrected by subtraction of the spectrum of the buffer (10 mM phosphate, 0.1 M NaCl) and the spectra are reported without smoothing.

Time resolved fluorescence was collected with a streak camera detection system (Hammamatsu C4334) coupled to a frequency-doubled cavity-dumped titanium–sapphire oscillator that provided excitation pulses at 391 nm. Spectra were collected from 450 to 600 nm, encompassing the entire fluorescence band of PerA, peaked at ~500 nm. Fluorescence lifetimes were determined using the integrated intensity from 475–525 nm and by nonlinear least-squares fitting to a convolution of the instrument response of the streak camera with an exponential decay function. The temporal instrument response was 0.03 ns for fast kinetics (<1 ns) and 0.75 ns for slower kinetics.

Femtosecond transient absorption measurements were obtained using an instrument outfitted with a CCD array detector for the collection of spectral data at multiple delay times following photoexcitation of the sample.[56] The total instrument response for the pump–probe experiments was 150 fs. Typically 5 s of averaging was used to obtain the transient spectrum at a given delay time. Cuvettes with a 2 mm path length were used and the samples were irradiated with 0.5 μJ/pulse focused to a 200-μm spot. The optical density at λ_{ex} was kept between 0.2 and 0.4. Analysis of the kinetic data was performed at multiple wavelengths using a Levenberg–Marquardt nonlinear least-squares fit to a general sum-of-exponentials function with an added Gaussian instrument response function.

Electrochemical measurements were performed using a CH Instruments Model 660A electrochemical workstation. The solvent was dimethylsulfoxide containing 0.1 M tetra-*n*-butylammonium perchlorate electrolyte. A 1.0 mm diameter platinum disk electrode, platinum wire counter electrode, and Ag/Ag_xO reference electrode were employed. The ferrocene/ferrocinium (Fc/Fc^+, 0.52 vs SCE) was used as an internal reference for all measurements. Spectroelectrochemical measurements were performed in the homemade quartz cell consisting of a 1 mm path length rectangular screw top spectrophotometric cuvette that is screwed into the bottom of a Teflon beaker. Platinum gauze, 100 mesh, woven from 0.07 mm diameter wire was used as a transparent working electrode. The electrode was placed in the 1 mm spectrophotometric cell and connected to the potentiostat output by a platinum wire. The platinum wire counter and silver wire reference electrodes were placed in the Teflon reservoir, which held a solution of 0.1 M tetra-*n*-butylammonium perchlorate. The electrochemical workstation controlled the potential of the working electrode, and a Shimadzu 1610A UV–VIS spectrometer obtained the absorption spectra of the redox species. All electrochemical measurements were carried out under a blanket of argon. A series of absorption spectra of the samples were taken until the potential induced spectral evolution was complete, which usually took 7 or 8 min.

4.1.1. N^3,N^9-Bis(3-hydroxypropyl)perylene-3,9-dicarboxamide (PerA). To a refluxing suspension of perylene-3,9-dicarboxylic acid diisobutyl ester (TCI American, 0.35 g, 0.78 mmol) in 10 mL tetrahydrofuran was added 3-hydroxypropylamine (7 mL, 0.09 mol) and catalytic sodium azide.[38] The solution became clear after several hours. Refluxing was continued for 60 h, at which time no starting material was detected by TLC. After cooling, a yellow powder precipitated and was filtered and dried (0.26 g, 74%). ^{1}H NMR (DMSO-d_6, 500 MHz) δ 1.76 (4H, m), 3.41 (4H, t),

3.57 (4H, t), 4.57 (2H, s), 7.61–8.61 (10H, m). MS: *m/z* 454.5 (M^+calcd). The diol was converted without further purification to its mono-DMT derivative in 35% yield following the method of Letsinger and Wu.[37] MS: *m/z* 757.2 (M^+calcd 756.9). The mono-DMT derivative was converted to its cyanoethyl-*N,N*-diisopropyl phosphoramidite derivative immediately prior to use in the preparation of conjugates **1–7** (Chart 2). Linker diols were incorporated into the conjugates using conventional solid-supported phosphoramidite synthesis. The conjugates were first isolated as trityl-on derivatives by RP HPLC and then detritylated in 80% acetic acid for 30 min and repurified by HPLC. Structures were confirmed by ES-MS and the purities were assured by analytical HPLC.

Acknowledgements

The authors thank Pierre Daublain for kinetic fitting and Michael Fuller for electrochemical measurements. This research is supported by the Division of Chemical Sciences, Office of Basic Energy Sciences, U.S. Department of Energy under Contracts DE-FG02-96ER14604 (F.D.L.) and DE-FG02-99ER14999 (M.R.W.).

References and notes

1. Nordlund, T. M.; Andersson, S.; Nilsson, L.; Rigler, R.; Graeslund, A.; McLaughlin, L. W. *Biochemistry* **1989**, *28*, 9095–9103.
2. O'Neil, M. A.; Barton, J. K. *J. Am. Chem. Soc.* **2004**, *126*, 11471–11483.
3. Kool, E. T. *Acc. Chem. Res.* **2002**, *35*, 936–943.
4. Zhang, L.; Long, H.; Boldt, G. E.; Janda, K. D.; Schatz, G. C.; Lewis, F. D. *Org. Biomol. Chem.* **2006**, *4*, 314–322.
5. Netzel, T. L.; Zhao, M.; Nafisi, K.; Headrick, J.; Sigman, M. S.; Eaton, B. E. *J. Am. Chem. Soc.* **1995**, *117*, 9119–9128.
6. Nakatani, K.; Dohno, C.; Saito, I. *J. Am. Chem. Soc.* **1999**, *121*, 10854–10855.
7. Okamoto, A.; Kanatani, K.; Saito, I. *J. Am. Chem. Soc.* **2004**, *126*, 4820–4827.
8. Amann, N.; Pandurski, E.; Fiebig, T.; Wagenknecht, H.-A. *Angew. Chem., Int. Ed.* **2002**, *41*, 2978–2980.
9. Hurley, D. J.; Tor, Y. *J. Am. Chem. Soc.* **2002**, *124*, 13231–13241.
10. Dogan, Z.; Paulini, R.; Rojas Stütz, J. A.; Narayanan, S.; Richert, C. *J. Am. Chem. Soc.* **2004**, *126*, 4762–4763.
11. Lai, J. S.; Qu, J.; Kool, E. T. *Angew. Chem., Int. Ed.* **2003**, *42*, 5973–5977.
12. Letsinger, R. L.; Wu, T. *J. Am. Chem. Soc.* **1994**, *116*, 811–812.
13. Salunkhe, M.; Wu, T.; Letsinger, R. L. *J. Am. Chem. Soc.* **1992**, *114*, 8768–8772.
14. Lewis, F. D.; Letsinger, R. L.; Wasielewski, M. R. *Acc. Chem. Res.* **2001**, *34*, 159–170.
15. Lewis, F. D.; Liu, X.; Wu, Y.; Miller, S. E.; Wasielewski, M. R.; Letsinger, R. L.; Sanishvili, R.; Joachimiak, A.; Tereshko, V.; Egli, M. *J. Am. Chem. Soc.* **1999**, *121*, 9905–9906.
16. Lewis, F. D.; Wu, T.; Zhang, Y.; Letsinger, R. L.; Greenfield, S. R.; Wasielewski, M. R. *Science* **1997**, *277*, 673–676.
17. Bevers, S.; O'Dea, T. P.; McLaughlin, L. W. *J. Am. Chem. Soc.* **1998**, *120*, 11004–11005.
18. Egli, M.; Tereshko, V.; Mushudov, R.; Sanishvili, R.; Liu, X.; Lewis, F. D. *J. Am. Chem. Soc.* **2003**, *125*, 10842–10849.
19. Lewis, F. D.; Zhang, L.; Liu, X.; Zuo, X.; Tiede, D. M.; Long, H.; Schatz, G. S. *J. Am. Chem. Soc.* **2005**, *127*, 14445–14453.
20. Ferentz, A. E.; Verdine, G. L. *J. Am. Chem. Soc.* **1991**, *113*, 4000–4002.
21. Rumney, S.; Kool, E. T. *J. Am. Chem. Soc.* **1995**, *117*, 5635–5646.
22. Yoshizawa, S.; Kawai, G.; Watanabe, K.; Miura, K.; Hirao, I. *Biochemistry* **1997**, *36*, 4761–4767.
23. Lewis, F. D.; Wasielewski, M. R. *Top. Curr. Chem.* **2004**, *236*, 45–65.
24. Lewis, F. D.; Wu, Y. *J. Photochem. Photobiol. C: Photochem. Rev.* **2001**, *2*, 1–16.
25. Takada, T.; Kawai, K.; Cai, X.; Sugimoto, A.; Fujitsuka, M.; Majima, T. *J. Am. Chem. Soc.* **2004**, *126*, 1125–1129.
26. Takada, T.; Kawai, K.; Fujitsuka, M.; Majima, T. *Angew. Chem., Int. Ed.* **2006**, *45*, 120–122.
27. Lewis, F. D.; Liu, X.; Miller, S. E.; Hayes, R. T.; Wasielewski, M. R. *J. Am. Chem. Soc.* **2002**, *124*, 14020–14026.
28. Lewis, F. D.; Liu, X.; Miller, S. E.; Wasielewski, M. R. *J. Am. Chem. Soc.* **1999**, *121*, 9746–9747.
29. Bevers, S.; Schutte, S.; McLaughlin, L. W. *J. Am. Chem. Soc.* **2000**, *122*, 5905–5915.
30. Lewis, F. D.; Kalgutkar, R. S.; Wu, Y.; Liu, X.; Liu, J.; Hayes, R. T.; Wasielewski, M. R. *J. Am. Chem. Soc.* **2000**, *122*, 12346–12351.
31. Zheng, Y.; Long, H.; Schatz, G. S.; Lewis, F. D. *Chem. Commun.* **2005**, 4795–4797.
32. Lewis, F. D.; Zhang, L.; Zuo, X. *J. Am. Chem. Soc.* **2005**, *127*, 10002–10003.
33. Lewis, F. D.; Wu, T.; Liu, X.; Letsinger, R. L.; Greenfield, S. R.; Miller, S. E.; Wasielewski, M. R. *J. Am. Chem. Soc.* **2000**, *122*, 2889–2902.
34. Lewis, F. D.; Zhang, Y.; Liu, X.; Xu, N.; Letsinger, R. L. *J. Phys. Chem. B* **1999**, *103*, 2570–2578.
35. Lewis, F. D.; Liu, J.; Weigel, W.; Rettig, W.; Kurnikov, I. V.; Beratan, D. N. *Proc. Natl. Acad. Sci. U.S.A.* **2002**, *99*, 12536–12541.
36. Daublain, P.; Lewis, F. D., unpublished results.
37. Letsinger, R. L.; Wu, T. *J. Am. Chem. Soc.* **1995**, *117*, 7323–7328.
38. Högberg, T.; Stroem, P.; Ebner, M.; Raemsby, S. *J. Org. Chem.* **1987**, *52*, 2033–2036.
39. Berlman, I. B. *Handbook of Fluorescence Spectra of Aromatic Molecules*, 2nd ed.; Academic: New York, NY, 1971.
40. Halasinski, T. M.; Weisman, J. L.; Ruiterkamp, R.; Lee, T. J.; Salama, F.; Head-Gordon, M. *J. Phys. Chem. A* **2003**, *107*, 3660–3669.
41. Hochstrasser, R. M. *J. Chem. Phys.* **1964**, *40*, 2559–2564.
42. Singh, A. K.; Mondal, J. A.; Ramakrishna, G.; Ghosh, H. N.; Bandyopadhyay, T.; Palit, D. K. *J. Phys. Chem. B* **2005**, *109*, 4014–4023.
43. Knibbe, H.; Rehn, D.; Weller, A. *Ber. Bunsen-Ges. Phys. Chem.* **1968**, *72*, 257–263.
44. Bloomfield, V. A.; Crothers, D. M.; Tinoco, I., Jr. *Nucleic Acids, Structures, Properties, Functions*; University Science Books: Sausalito, CA, 2000.
45. Johnson, W. C. *Electronic Circular Dichroism Spectroscopy of Nucleic Acids*; Saenger, W., Ed.; Landolt-Börnstein, Group VII; Springer: Berlin, 1990; Vol. I, pp 1–24.
46. Ardhammar, M.; Kurucsev, T.; Nordén, B. DNA–Drug Interactions. In *Circular Dichroism, Principles and Applications*; Berova, N., Nakanishi, K., Woody, R. W., Eds.; Wiley-VCH: New York, NY, 2000; pp 741–768.

47. Koberle, K.; Schlichting, O. U.S. Patent, 1941, 11335.
48. Lewis, F. D.; Zhu, H.; Daublain, P.; Fiebig, T.; Raytchev, M.; Wang, Q.; Shafirovich, V. *J. Am. Chem. Soc.* **2006**, *128*, 791–800.
49. Weller, A. *Zeit. Phys. Chem. Neue. Folg.* **1982**, *133*, 93–98.
50. Seidel, C. A. M.; Schulz, A.; Sauer, M. H. M. *J. Phys. Chem.* **1996**, *100*, 5541–5553.
51. Schmidt, J. A.; McIntosh, A. R.; Weedon, A. C.; Bolton, J. R.; Connolly, J. S.; Hurley, J. K.; Wasielewski, M. R. *J. Am. Chem. Soc.* **1988**, *110*, 1733–1740.
52. Verhoeven, J. W. *J. Photochem. Photobiol., C* **2006**, *7*, 40–60.
53. Hess, S.; Götz, M.; Davis, W. B.; Michel-Beyerle, M. E. *J. Am. Chem. Soc.* **2001**, *123*, 10046–10055.
54. Lewis, F. D.; Daublain, P.; Delos Santos, G.; Liu, W.; Asatryan, A. M.; Markarian, S. A.; Fiebig, T.; Raytchev, M.; Wang, Q. *J. Am. Chem. Soc.* **2006**, *128*, 4792–4801.
55. Sjoeback, R.; Nygren, J.; Kubista, M. *Spectrochim. Acta, Part A* **1995**, *51*, L7–L21.
56. Kelley, R. F.; Tauber, M. J.; Wasielewski, M. R. *J. Am. Chem. Soc.* **2006**, *128*, 4779–4791.